Reliability of micro-BGA-on-Flex Assemblies

Robert Larmouth, James Keating
Teledyne Electronic Technologies
110 Lowell Rd.
Hudson, NH 03051
Phone: (603) 889-6191 FAX (603) 882-4457

Abstract

Ball Grid Array (BGA) packages offer increased I/O density with relatively coarse pitches, when compared to peripheral-leaded SMT packages of the same I/O count. Although the question "Does the lack of a compliant lead in the BGA solder joint reduce reliability?" continues to be asked, there is evidence of steady industry acceptance of this technology. Micro-BGA technology, one example of chip-scale packaging, is an extension of this technology which allows designers to approach multi-chip module densities while continuing to employ surface mount assembly techniques. The reliability concern, however, is exaggerated since the volume of solder decreases with the finer pitch micro-BGA devices. At the same time, increased use of surface mount on flex circuits, particularly in small form factor products, is demonstrating the ability of flex to mitigate the stress created in a solder joint during thermal excursions.

This paper summarizes work being done at Teledyne Electronic Technologies on assemblies employing microBGA packages on both rigid and flexible substrates. These assemblies include BGA pitches down to 0.5mm and pad diameters down to 0.3mm. Solder joint fatigue and/or cracking as a potential failure mechanism is examined, and reliability analysis data is presented as part of an overall assessment of the microBGA technology for use in products in the medical and communications markets. (Keywords: microBGA, flex, SMT-on-Flex, microvia, solder joint reliability, CSP)

INTRODUCTION

Background: SMT-on-Flex

The use of flex based interconnects has been steadily increasing, primarily as a result of the demand for systems which are smaller, lighter, and offer higher performance at an affordable price. Flex based assemblies can be extremely thin and compliant, and can further reduce weight, space and cost by the elimination of components such as connectors. Long used strictly as a cable or interconnection between rigid board assemblies, flex is now playing a more active role as a packaging/assembly alternative by the addition of surface mount devices directly to the flex substrate. The camcorder is a good example of the use of SMT-on-flex in high volume commercial applications. SMT devices are typically traditional packaged leaded devices such as QFPs or TSOPs, but applications requiring chip on flex (COF), either as chip and wire assemblies or flip chip on flex (FCOF), are growing rapidly. The disk drive industry has been steadily increasing the demands for COF and FCOF assemblies, particularly for high performance MR drives. In these applications, the traditional leaded package may fall short of the low-weight/volume and high-electrical/thermal performance goals. Users of flip-chip, however, report the need for underfill materials to achieve acceptable reliability levels, almost always on rigid boards and sometimes on flex, although the latter is often more reliable. [1,2]

Other factors need to be considered, however, with respect to the design and assembly processes. To ensure optimal solder joint geometry and process yields in SMT-on-flex applications, special stiffening of the substrate may be required for SMT attachment to the circuit. Materials such as aluminum or plastic are often used to provide localized stiffening of selected areas during assembly.[3] These stiffeners would need to be applied during the fabrication by the flex circuit vendor and tend to add to the cost of the substrate. They may also reduce the inherent advantages of compliance in the flex substrate over the life of the product. In other cases special handling or fixturing may be necessary to hold the substrate flat during the assembly and reflow operations. Temporary stiffening, such as a picture frame or clamping, can be used during the assembly process to hold the substrate [3].

Just as they have for rigid board applications, BGAs and chip scale packages are beginning to fill a gap between traditional SMT and bare die for flex assemblies. BGAs and microBGAs can approach the performance and space savings afforded by bare die while retaining surface mount assembly processes, but reliability is still sometimes questioned by potential users. Assemblers would rather not be forced to use underfill materials to ensure solder joint reliability, as is often the case in flip chip applications. Again, flex figures into the equation for new applications where reliability is of utmost importance. Studies have shown that SMT solder joints on flex can withstand thousands of thermal cycles [4] and that they are often more reliable than their rigid board counterparts [5], since the compliant nature of flex tends to decouple the stress caused by the so-called "global" mismatch between packages and the substrate to which they are assembled. Flex can further improve reliability by reducing stress caused by “local” mismatch - that between the solder itself and the substrate.

µBGA-on-Flex Project Objectives

As mentioned above, there is ample evidence in the literature of the reliability of SMT-on-flex, however the vast majority of these data do not include the newer micro-BGA and other chip scale SMDs. This fact creates the rationale for the work reported herein. The objectives of the Micro-BGA-on-Flex Project at Teledyne are threefold:

- establish reliability projections for microBGA devices on flex and thin PWB assemblies
- confirm reliability levels via physical testing of test vehicle assemblies
- determine ease of assembly (e.g., are stiffeners for flex and/or underfill for packages required?)

The scope of this paper encompasses the first objective, and addresses the approach taken for the second and third objectives.

MEDICAL MICROELECTRONICS REQIREMENTS

As a manufacturer of microelectronics for medical implantable and wearable products, Teledyne is keenly aware of the drive to reduce the weight and size of these and other products (hand-held, for example) while increasing the performance and reliability. In the case of pacemakers, for example, size and weight are crucial, as these factors directly impact the extent of the surgery required for the implant and may ultimately affect the compatibility with a given patient. Pacemakers are now approaching a thickness of about 0.320” (8mm) and a weight of ½ oz. (12-15 gm). This form factor, coupled with the demand for increased performance such as memory capacity, result in a requirement for extremely low profile packaging. On the other hand, the medical industry tends to be conservative with respect to adoption of new technologies, particularly in the absence of extensive reliability test data and/or proven service records in other products. Once limited to hermetic ceramic hybrids, medical electronics manufacturers are now utlizing thin PWB cards and flex circuits, albeit ultimately contained in a titanium can. It behooves manufacturers such as Teledyne, then, to establish the reliability of new technologies as quickly as possible in the technology maturation cycle. The microBGA package is certainly a candidate for insertion into medical electronics, for the advantages stated above. Further, its implied compatibility with PWB and flex SMT assembly platforms make it attractive from a cost perspective.

The testing and reliability requirements for printed wiring boards used in implantable medical devices are based primarily on well known industry standards. The goal is to assure that the boards will withstand not only the intended application, which could be considered a relatively benign environment, but also the assembly and shipping processes and environments. Similarly, the microelectronic assembly also undergoes rigorous physical testing, not so much to simulate the operating environment, but to ensure high reliability levels of the components and interconnections. For this reason, many manufacturers base their qualification testing on MIL-STD-883, with the addition of selected board-level tests such as Thermal Stress (10 second solder float at 550° F to verify the ability to withstand most assembly processes). A typical qualification test flow for an implantable microelectronic package/assembly is shown in Table 1. (MATP is an internal diagnostic test.)

Sub group	Test name	Test Condition	Sample Size (accept qty)
C1	Initial Electrical	per MATP	5 (0)
“	External Visual	MIL-STD-883-2009	“
“	Temperature Cycle	MIL-STD-883-1010 -20 +85°C, 10 cycles	“
“	Constant Acceleration	MIL-STD-883-2002 2000g’s, Y1 direction	“
“	External Visual	MIL-STD-883-2009	“
“	Final Electrical	per MATP	“
C2	Initial Electrical	per MATP	22 (0)
“	Steady-State Life Test	MIL-STD-883-1005 1000 hours @ 125°C	“
“	Interim Electrical 168 hour int.	per MATP	“
“	Interim Electrical 504 hour int.	per MATP	“
“	Final Electrical	per MATP	“
C4	Internal Visual	MIL-STD-883-2014	2 (0)
“	Wirebond Strength	MIL-STD-883-2011 300°C Precond. Bake, Destructive Bond Pull	“
“	Element Shear	MIL-STD-883-2019	2 (0)

Table 1.
Typical Qualification Flow for Implantable Electronics

This type of qualification requirement is typical for new product designs. However, when new component, packaging, or assembly technology is introduced, the test regimens tend to be more severe. For example, manufacturers often increase the temperature cycling extremes to -55 to +125°C (MIL-STD-883, Condition 3) when qualifying new device package types such as a BGA. It is this requirement which reflects one of the major concerns in the medical implantables field - the robustness and long term reliability of micro-interconnections. When considering the newer microBGA packaging technology for insertion into this type of application, a logical choice for assessing the interconnection reliability in this context was the Tessera TV46 microBGA. Before incurring the expense of building and testing assemblies, however, it was reasoned that basic expectations of reliability could be gleaned from adaptation of widely used analytical models for solder joints.

SOLDER JOINT RELIABILITY MODEL

Analysis Approach and Assumptions

In work previously reported by the authors [6], microvia-in-pad technology was employed in an MCM-L substrate to allow for routing of the wirebond pads to a high density signal layer. This construction had first been rendered as a two-layer flex with soldered components, wherein the volume of the microvia was relatively small compared to the total solder volume, thereby alleviating any concerns regarding reduced solder joint quality as a result of solder flowing into the microvia. In fact, the solder joint integrity appeared to be enhanced by the addition of this short column of solder. Although the TV46 microBGA has a relatively low I/O density, the use of multiple packages could create routing density challenges in certain applications. It was therefore decided that this feature be incorporated into the present reliability assessment.

The first step in the reliability assessment was to develop an analytical model to determine the relative reliability of the TV46 microBGA solder joints on various Teledyne pad and substrate configurations. The model was developed to address assembly of the TV46 onto four different substrate configurations:

1. double-sided flex with standard 0.012” (0.3mm)pads
2. same as 1 but with 0.004” (0.1mm) microvias in the pads
3. double-sided FR4 laminate 0.030” (0.75mm) thick with standard 0.012” (0.3mm) pads
4. same as 3 but with 0.004” (0.1mm) microvias in the pads

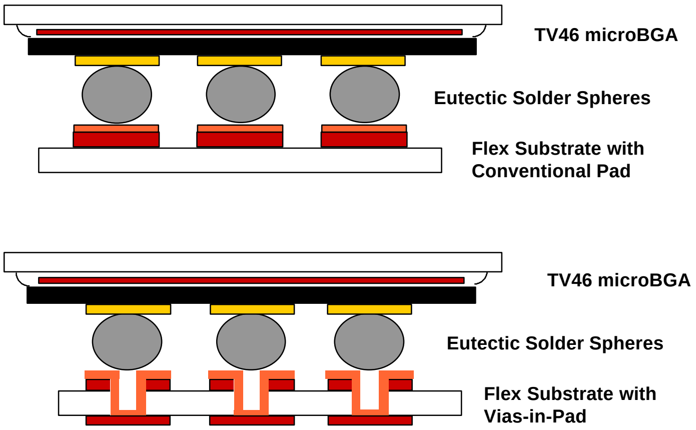

Figure 1. Schematic of uBGA Attachment
Top: Configuration 1; Bottom: Configuration 2

Configurations 1 and 2 are depicted in Figure 1. The model also took into consideration the following additional design data:

- TV46 pad diameter (2R): 0.012” (0.3mm)
- TV46 solder ball diameter (2r): 0.013” (0.33mm)
- HASL thickness (avg) on substrate: 0.0003” (0.075mm)
- Additional solder vol. in microvias: 16 mils^3 (2.62x10^{-7}cm^3)
- TV46 die is unconstrained , to the extent allowed by the package design [7]
- Manufacturing processes well-established (i.e. Weibull slope m=3)

In the analysis, the microBGA solder joint is represented with a three-disk axisymmetrical model corresponding to the structure shown in figure 1, where the top disk is the pad attached to the TV46, the center disk is the solder joint (as reflowed) and the bottom disk is the pad attached to either the flex or PWB. The approach is to derive the cycles to failure based on calculated stress, not strain, since most of the material properties and dimensions are well-defined, following reference [8]. Figure 2 is the free body diagram (from the three-disk model) which determines the entries for the 4x4 matrix used to calculate the local mismatch stress.[9] The mean number of cycles to failure is based on the Paris-Erdogan relation and checked by the Coffin-Manson law.

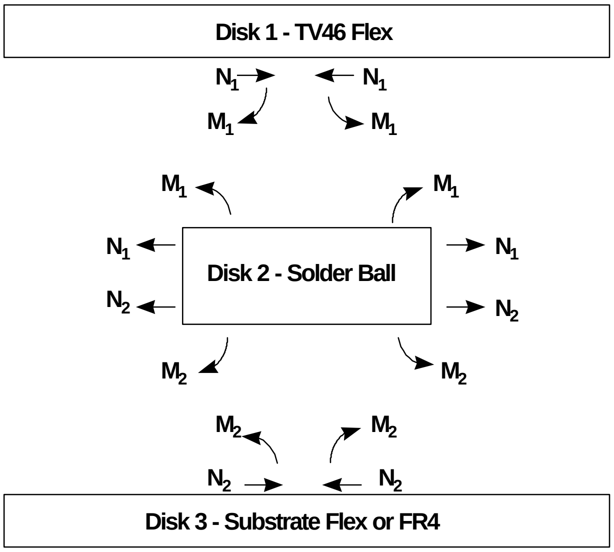

Figure 2.
Free Body Diagram

The global mismatch is characterized by the value:

$$\Delta u = [\alpha_{dev}\Delta T^{o}_{dev} - \alpha_{subs}\Delta T^{o}_{subs}]L$$

where L is the distance from the device center to the corner solder joint, and *dev* and *subs* refer to the TV46 device and the flex substrate, respectively. The solder failure indicator (stress) is then expressed as:

$$\textit{stress} = K_1 \beta \Delta u$$

where β depends on compliance of the device and substrate and K_1 depends on solder geometry and its properties. For the unconstrained die condition as noted above, the value of u approaches zero, since the flex in the package and the flex in the substrate behave similarly, and the ΔT values are equal. Note that this would not be true in the case of device power cycling, where ΔT_{dev} would not be equal to ΔT_{subs}. The failure indicator, then, is predominantly dependent on local mismatch, the latter given by:

$$\textit{stress} = K_2(\alpha_{solder} - \alpha_{subs})\, \Delta T^o$$

where K_2 depends on solder joint geometry and its mechanical properties.

Modeling Results

The stress calculations are shown in Appendix A, for which a Fortran code was written to generate the results shown in Table 2.

Parameter	(A) -55°/ +85°C			
	Flex Substrate		FR4 PWB	
	Pad	Pad+ via	Pad	Pad+ via
Shear stress caused by local mismatch (τ_{local}, psi)	479		586	
Peeling stress caused by local mismatch (σ_{local}, psi)	624		602	

Parameter	(B) -55°/ +125°C			
	Flex Substrate		FR4 PWB	
	Pad	Pad + via	Pad	Pad+ via
Shear stress caused by local mismatch (τ_{local}, psi)	615		754	
Peeling stress caused by local mismatch (σ_{local}, psi)	802		775	

Parameter	(C) -55°/ +125°C	
	Flex Substrate	FR4 PWB
	Constrained die	Constrained die
Shear stress caused by local mismatch (τ_{local}, psi)	2,582	3,411
Peeling stress caused by local mismatch (σ_{local}, psi)	11,028	14,582

Table 2.
Results of Stress Calculations

The top and middle sections of table 2 show the calculated stresses at two different temperature extremes for both substrate configurations. The +85^{o}C extreme reflects the normal qualification requirement while the +125^{o}C extreme reflects a more widely accepted value for solder joint reliability testing. The bottom section, shown strictly for comparison, is calculated assuming there was no stress decoupling of the die in the package. That is, these values would approximate those calculated for a flip chip application where no underfill had been used. The relatively low stresses in the flex half of the top two sections reflect the fact that the global mismatch is near zero, based on the decoupling effect of the TV46 plus the similarity in the behavior of the package flex and substrate flex, as noted earlier. In Table 3, the cycles-to-failure are calculated as shown in Appendix A.

Parameter	(A) -55°/ +85°C			
	Flex Substrate		FR4 PWB	
	Pad	Pad+ via	Pad	Pad+ via
Mean # cycles to failure	27,820	30,090	15,190	16,430
Expected Failure Rate (ppm) of 46 ball circuits after 100 cycles (m=3)	1	1	9	7

Parameter	(B) -55°/ +125°C			
	Flex Substrate		FR4 PWB	
	Pad	Pad + via	Pad	Pad+ via
Mean # cycles to failure	13,140	14,210	7,130	7,720
Expected Failure Rate (ppm) of 46 ball circuits after 100 cycles (m=3)	14	11	88	69

Parameter	(C) -55°/ +125°C	
	Flex Substrate	FR4 PWB
Mean # cycles to failure	Constrained die	Constrained die
	178	77
Expected Failure Rate (ppm) of 46 ball circuits after 100 cycles (m=3)	100%	100%

Table 3.
Results of Cycles-to-Failure Calculations

The data in Table 3 is organized as in Table 2, except that there are values unique to each of the four attachment configurations. Note that the calculations assume a stable, low-defect manufacturing process. Overall, the data clearly shows the higher reliability expected for attachment to flex as compared to FR4 boards. At the 125^{o}C test condition, the values obtained for the flex substrate compare favorably to values reported by industry experts [8] for conventional (e.g. PQFP) leaded SMT packages on FR4. The values obtained for the FR4 substrate, while only about half of those for flex, still fall in the range of data reported. Reference [8] cites cycles-to-failure values as low as 500 for low profile QFP-type packages on thick boards and as high as 12,000 for low lead-count devices with higher profiles of 0.60” (15mm) height. Finally, the microvia-in-pad design offers a slight improvement in reliability, primarily because of its interruption of the potential crack propagation path. Again, the bottom section of the table is provided for purposes of comparison to a flip-chip attachment without underfill, and these predicted cycle-to-failure values exhibit good agreement with actual test data reported recently in the literature [11].

The combination of the calculated stress and cycle-to-failure data provided sufficient evidence that the µBGA package attachment should be reliable on both flex and thin FR4, thereby justifying continuation of the project to the physical assembly and testing phases.

µBGA-ON-FLEX ASSEMBLY

Test Vehicle Description

The Tessera TV46 CSP package configuration is being introduced for flash memory with several end users. Such a form factor, particularly for SRAM and DRAM CSPs, is directly applicable to various microelectronics designs under development by Teledyne for medical implantables and wearables. The test vehicle substrate design is a modification of the Tessera TV46 test coupon. The design has .006” (0.15mm) lines and spaces with .012”∅ (0.3mm) capture pads for the µBGA solder balls to align and be soldered. The lines are connected together in a daisy chain to allow for evaluation of all test points.

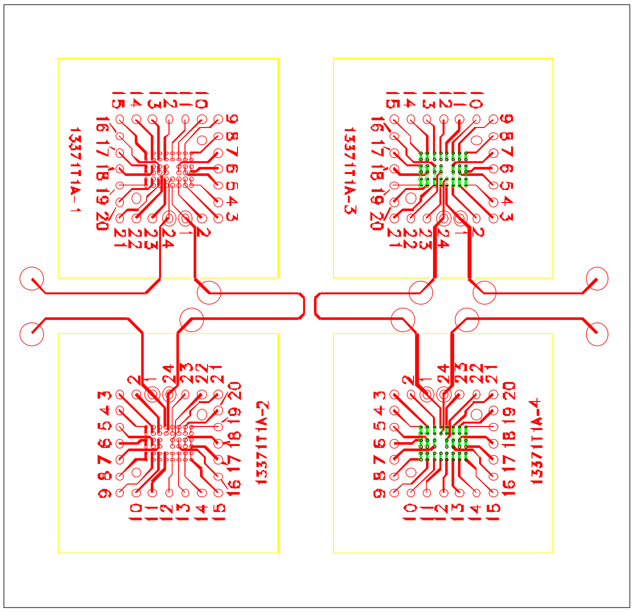

Figure 3.
µBGA Assembly Test Vehicle Layout

The design layout (shown in Figure 3) also supports isolated testing of individual test points to troubleshoot electrical opens or shorts. Each part has four TV46 attachment sites. Modifications by Teledyne included separating the four parts into two pairs, one of which would include through hole via routing. The design now will accommodate the assembly and testing of µBGA CSPs to both a single layer pad design and a plated through hole microvia design. The objective is to determine actual solder joint dimensional and geometric data to feed back into the analytical model for ‘tweaking’, and then to verify the reliability levels of the various configurations. The Tessera packages supplied are both mechanical units used for solder joint integrity evaluation and daisy chain configuration for electrical continuity monitoring. The surface finish on the substrates is a eutectic HASL finish with an average thickness of 0.0004”. Figure 4 is a cross-sectional view of both pad types on a finished flex substrate.

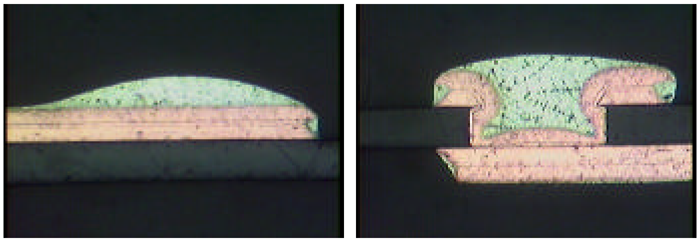
Conventional Pad
(Daisy chain trace on left)

Microvia-in-Pad
(Daisy chain trace on layer 2)

Figure 4.
Cross-section of Flex Test Vehicle after HASL

Assembly Characterization

Assembly of the TV46 CSPs to the flex test substrate was accomplished utilizing a Conceptronics BGA hot-air reflow station without the need for added solder paste. The flex was held flat with a specially designed vacuum fixture while the TV46 devices were aligned via a split-optics system and placed with a vacuum nozzle. Solder ball collapse was controlled by the available wettable pad areas on the device and the flex substrates. Initial prototypes assembled fairly easily with no major defect problems noted.

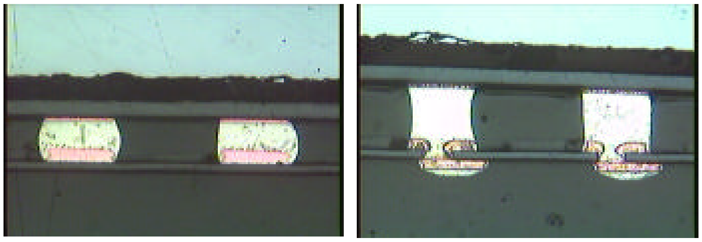

Figure 5.
Cross-sections of Assembled Test Vehicle Solder

Joints for Conventional (left) and microVia (right) pads

Figure 5 shows cross-sections of two sections of an assembled test vehicle, one of the conventional pad site and one of the microvia-in-pad site. The former exhibits uniform solder joints with a thickness very close to the predicted 0.0007". The latter exhibits a taller solder joint, appearing to contain a larger volume of solder. At the time of this writing, an insufficient number of assemblies has been completed to acquire a statistical view of this difference, but one possible explanation is that the conventional pad site is effectively enlarged by the adjoining daisy chain trace to the extent of the soldermask opening, while the microvia-in-pad site has no traces on the same plane. The conventional pad therefore has a larger area over which to distribute the available solder. One must keep in mind the fact that the TV46 solder ball volume is significantly larger than that added by the HASL process. Future substrates will be characterized to verify the actual solder volumes and reason for the height differences. Nonetheless, the initial assembly does indicate the ability to control the solder collapse through the pad and soldermask design. The vacuum fixture also illustrated at least one approach to stabilizing the flex for assembly without the use of either permanent or temporary stiffeners. This approach would have to be further proven and perhaps modified for high volume manufacturing.

Reliability Testing

Although qualification tests as outlined in Table 1 will ultimately be performed as part of any new product introduction, a number of reliability tests designed to establish confidence levels for this technology are planned, using the assembled test vehicles. As implied earlier, the focus is on temperature cycling using the more aggressive cycle of -55 to +125°C. Electrical continuity will be monitored in-situ through the daisy chain circuits with data collected at both temperature extremes. Power cycling is also planned, subject to the type of device being packaged for a specific application. Component shear and/or pull tests will be performed, primarily to establish a baseline for overall mechanical integrity of the interconnections as compared to other interconnections such as wirebonds, bare die attach, epoxy-mounted passives and leaded SMT solder joints. Customer-specified board-level tests such as Surface Insulation Resistance may be incorporated into the plan. Finally, mechanical shock will be performed per MIL-STD-883, most likely only for special conditions requested by medical customers.

SUMMARY

As part of an effort to evaluate the applicability of microBGA packaging to implantable medical and other similar electronic assemblies, an analytical model has been adapted to proposed solder attachment structures for both flexible and rigid PWB substrates. The modeling results show that solder joint reliability through temperature cycling is predicted to be significantly higher for microBGAs on flex than for the same package on 0.030" thick FR4 boards. The maximum number of 14,210 cycles-to-failure for the flex configuration compares favorably with the most compliant leaded SMT devices reported in the literature. The 7,720 cycles-to-failure predicted for the FR4 PWB configuration, while only about half that of the flex configuration, is still considered to be acceptable for the intended applications. The microvia-in-pad design is shown to slightly improve the reliability for both flex and FR4, allowing it to be considered for higher density routing designs. Moreover, the data suggest that underfill is not needed for attachment of this specific type of package when considering a stable, low defect rate manufacturing process. This may not be true, however, for certain device types where power cycling is a more representative test for solder joint life.

The initial assembly results indicate acceptable quality for the HASL-finished substrates; other finishes should be considered but are not within the scope of this project. Ongoing assembly work will serve to fully characterize the attachment process in an effort to optimize the solder joint dimensions and geometry, after which a suitable number of assemblies will be built for physical reliability testing as discussed in the previous section.

REFERENCES:

[1] J. Fjeldstad and T. DiStefano, "Flex on Chip for High Density Chip Packaging" in Proc. IPC National Flex Conference, 1995.

[2] M. Bottcher, et al, "High Density Flexible Circuits with Solder Ball Arrays", in Proc. Flexcon '94

[3] T. Patterson, "Design Considerations for Flip Chip on Flex." In Proc. Flexcon '95, Sunnyvale, CA.

[4] J. Fjeldstad, "Design Considerations for Surface Mount on Flexible Circuitry", PC Fab, pp 106, 115-121, October, 1989.

[5] K. Gilleo, "SMT + Flex = Maximum Versatility and Reliability", Electronic Packaging & Production, pp 56-59, July, 1992.

[6] R. Larmouth and J. Keating, "High Density SMT Assemblies Based on Flex Substrates", in Proc. Surface Mount International, September, 1996.

[7] J. Fjeldstad and M. Perry, "Finite Element Analysis of a Compliant Chip Scale Ball Grid Array Package", in Proc. CHIPCON, February 1996.

[8] B. Mirman, "Comparative Analysis of Solder Stresses of μBGA Under Temperature Cycling", report prepared for Teledyne Electronic Technologies, July, 1997.

[9] S.Timoshenko and S. Woinowski-Krieger, “Theory of Plates and Shells”, McGraw-Hill, 1959.

[10] C-Y. Li, R. Subrahmanyan, J.R. Wilcox, D. Stone, “A Damage Integral Methodology for Thermal and Mechanical Fatigue of Solder Joints”, *Solder Joint Reliability*, edited by John Lau, Van Nostrand, 1991.

[11] K. Casson, B. Gibson, “Flip-on-Flex: Solder Bumped ICs Bond to NovaClad®, a New High Temperature, Adhesiveless Flex Material”, Flexible Circuits Engineering, pp 9-11, August, 1995.

APPENDIX A

From the free body diagram:

$$\tau \left\{ \begin{matrix} M_1 \\ M_2 \\ N_1 \\ N_2 \end{matrix} \right\} = \left\{ \begin{matrix} 0 \\ 0 \\ (1 + v_1)\alpha_1 \Delta T^\circ{}_1 - (1 + v_2)\alpha_2 \, \Delta T^\circ{}_2 \\ (1 + v_3)\alpha_3 \Delta T^\circ{}_3 - (1 + v_2)\alpha_2 \, \Delta T^\circ{}_2 \end{matrix} \right\}$$

The first entry calculation with r = solder radius and R = pad radius is:

$$T_{11} = \frac{1 - v_1^2}{2E_1 t_1^3} \left\{ 1 + \frac{r^2}{R^2} \, \frac{1 - v_1}{1 - v_1} \right\} + \frac{1 - v_2^2}{E_2 t_2^3}$$

and so on...

The local shear stress is calculated by:

$$\tau_{local} = \frac{2max\,(|N_1|\,,|N_2|\,)}{r}$$

and the local peeling stress by:

$$\sigma_{local} = \frac{16max\,(|M_1|\,,|M_2|\,)}{r^2}$$

The Paris-Erdogan relation for crack propagation dependence on stress [10] is:

$$\frac{da}{dN} = B\,(\tau\sqrt{\pi\, a}\,)^{p}$$

where *a* = crack length,
N = number of cycles,
B and *p* are material characteristics

Plugging in calculated stress values and using known similar values for B, p:

$$N_f \geq 100\left(\frac{3127}{\tau}\right)^3$$

= number of cycles to failure

Failure rate calculation where 46 = number of solder joints, 17,040 = number of cycles and 3 = Weibull distribution

$$1 - (0.5)^{46x}\left(\frac{100}{17{,}040}\right)^3 = 6 \text{ X } 10^{-6}$$